DISRUPTION EVENT CHARACTERIZATION AND FORECASTING IN TOKAMAKS

EX/P6-26

S.A. SABBAGH*, J.W. BERKERY, Y.S. PARK, J.H. AHN, Y. JIANG, J.D. RIQUEZES
Columbia University
New York, NY, USA
*email: sabbagh@pppl.gov

R.E. BELL, M.D. BOYER, B.P. LEBLANC, C.E. MYERS, Z.R. WANG
Princeton Plasma Physics Laboratory
Princeton, NJ, USA

J.G. BAK, J. KIM, J. KO, W. KO, J.H. LEE, Y.K. OH, S.W. YOON
National Fusion Research Institute
Daejeon, Republic of Korea

J. HOLLOCOMBE, A. KIRK, L. KOGAN, A. THORNTON
Culham Centre for Fusion Energy, UKAEA
Abingdon, UK

A.H. GLASSER
Fusion Theory and Computation, Inc.
Kingston, WA, USA

Abstract

Disruption prediction and avoidance is a critical need for next-step tokamaks such as ITER. The Disruption Event Characterization and Forecasting Code (DECAF) is used to fully automate analysis of tokamak data to determine chains of events that lead to disruptions and to forecast their evolution allowing sufficient time for mitigation or full avoidance. Disruption event chains related to local rotating or global MHD modes and vertical instability are examined with warnings issued for many off-normal events including density limits, plasma dynamics, confinement transitions, and profile variations. Along with Greenwald density limit evaluation, a local radiative island power balance theory is evaluated and compared to the observation of island growth. Automated decomposition and analysis of rotating tearing modes produce physical event chains leading to disruptions. A total MHD state warning model comprised of 15 separate criteria produce a disruption forecast about 180 ms before a standard locked mode detector warning. Single DECAF event analyses have begun on KSTAR, MAST, and NSTX/-U databases with thousands of shot seconds of device operation using from 0.5 - 1 million tested sample times per device. An initial multi-device database comparison illustrates a highly important result that plasma disruptivity does not need to increase as β_N increases. Global MHD instabilities such as resistive wall modes (RWM) can give the least amount of warning time before disruption. In an NSTX database with unstable modes, the RWM onset, loss of boundary and current control, and disruption event warnings are found in all cases and vertical displacement events are found in 91% of cases. An initial time-dependent reduced physics model of kinetic RWM stabilization created to forecast the disruption chain predicts instability 84% of the time for experimentally unstable cases with relatively low false positive rate. Instances of disruption event chain analysis illustrate dynamics including H-L back transitions for rotating MHD and global RWM triggering events. Disruption warnings are issued with sufficient time before the disruption (on transport timescales) to potentially allow active profile control for disruption avoidance, active mode control, or mitigation.

1. INTRODUCTION

Disruption prediction and avoidance is a critical need for next-step tokamaks such as ITER, since plasma disruptions [1,2] can place significant thermal heat loads and electromagnetic forces on the device and can potentially lead to damage from runaway electrons [3]. Meeting these challenging goals with the high reliability required for ITER and future tokamaks goes beyond active instability control alone and will require multiple approaches, including an understanding of the connection between events leading to disruptions, and the ability to forecast such events well before they occur. The Disruption Event Characterization and Forecasting Code (DECAF), under development for this purpose, is used to automate analysis of tokamak data to determine chains of events that lead to disruptions and to forecast their evolution to inform plasma profile and mode control systems aimed to avoid, or if needed to mitigate the deleterious effects of a disruption. The events largely follow the paradigm established by the manual analysis performed by de Vries, et al. [4] for JET. DECAF further aims to automatically determine the relation of the events and quantify their appearance to characterize the most probable and deleterious event chains, and also to forecast the onset of the events and chains, especially for events that experimentally manifest in close time proximity to the disruption and would elude disruption

avoidance control systems, or even disruption mitigation systems. The DECAF paradigm is primarily physics-based and aims to provide a quantitative and, importantly, a deterministic (rather than a statistical) predictor for disruptions. It also aims to provide an understanding of the dynamics of the events leading to disruptions to best ensure disruption prediction extrapolability to future devices. This is highly important in high fusion power devices such as ITER in which the production of disruptions to teach purely automated model building approaches is highly restricted. Still, the DECAF approach and code are highly flexible and allow a large range of models from simple empirical comparisons, to reduced explicit analytic models based on computationally intensive first-principles physics analysis, or machine learning reductions of first-principles physics models. To best validate the expanding models continually being implemented in DECAF, significant effort is being placed on testing the algorithms against *full* tokamak databases on multiple tokamak devices throughout the world. As shown later, this approach is required to avoid errant determination of plasma parameters from databases limited to time periods that are only in close time proximity to the disruption. A larger variety of devices also provides essential depth in testing physics models and determining uniqueness and commonality in the events and their chains leading to disruptions. In the present work, the KSTAR, MAST, and NSTX/NSTX-U databases are examined, with analysis expanding to the DIII-D and TCV databases that are also available. The following sections examine an important subset of the event analysis in the code and insights gained on the connection of plasma dynamics to the events.

2. DISRUPTION CHAIN EVENTS AND WARNING LEVELS

Figure 1 simply illustrates the paradigm that DECAF follows in providing automated understanding of the dynamics leading to a tokamak disruption along with an example from experiment. Continuous tokamak plasma operation at high fusion performance is desired (Fig. 1a). However, at some point this "normal" operational plasma state can be altered by many different "events" ranging from purely technical aspects (e.g.

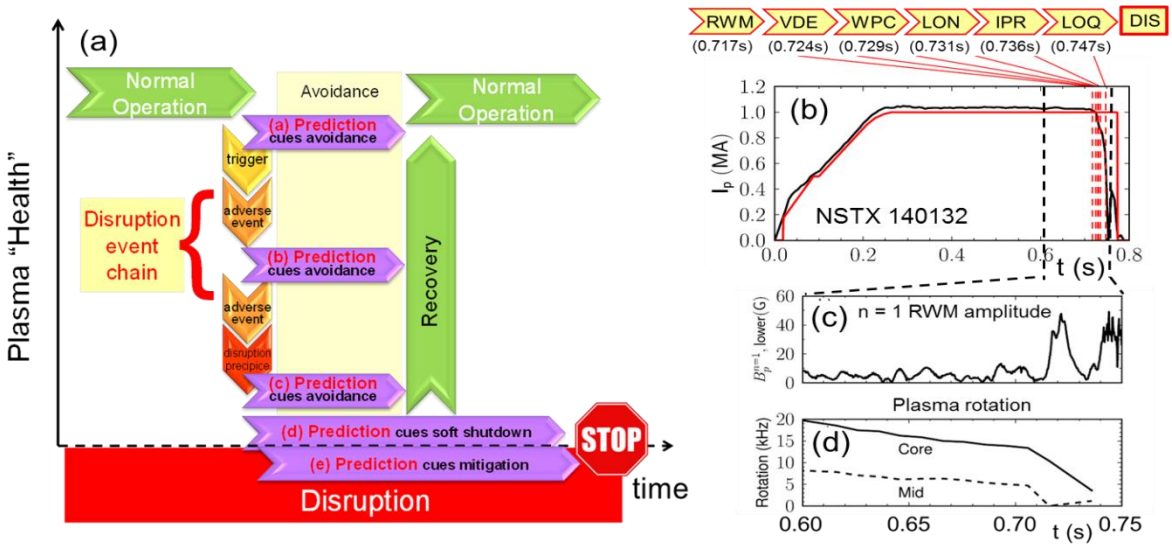

Fig. 1. (a) Schematic diagram illustrating a paradigm of plasma state evolution away from normal operation toward a plasma disruption as a series of events that form a disruption event chain, (b) automated evaluation of the disruption event chain for a plasma discharge with $\beta_N = 4.5$, (c) and (d) higher time resolution illustration of n = 1 RWM amplitude and plasma toroidal rotation as the disruption is approached.

magnetic field power supply interruption) to more complex reasons such as plasma instabilities. This alteration is considered as a chain of individual events, starting with a trigger event and evolving toward the plasma disruption (here labelled by the acronym DIS representing the plasma current quench). DECAF analysis of device databases aims to automatically determine and provide understanding of this chain of events. Future real-time implementations of DECAF diagnostic interpretation and forecasting models of such events can then be used to trigger disruption avoidance systems. This strategy can be contrasted to present disruption avoidance systems, e.g. MHD instability control [5] that essentially wait until the "disruption precipice" to address avoidance of the oncoming disruption. Figure 1b) shows a DECAF analysis of a plasma with "mid-range" normalized beta $\beta_N \equiv 10^8 <\beta_t> aB_0/I_p$ (where $\beta_t \equiv 2\mu_0 <p>/B_0^2 = 4.5$ toroidal beta, p is the plasma pressure, B_0 is the vacuum toroidal magnetic field at the plasma geometric center, and a is the plasma minor radius at the midplane) in NSTX. In this case, a global magnetohydrodynamic instability (resistive wall mode, RWM) is identified by DECAF as the event chain trigger, which is normally thought to be the direct precursor to the

disruption (DIS). However, DECAF identifies several interceding events. Next in the chain, 7 ms later, is a vertical displacement event (VDE). Five milliseconds later, a wall proximity warning (WPC) is issued indicating that the plasma boundary is about to touch the device first wall (and does soon after the warning). A low plasma density warning (LON) is issued 2 ms later, followed 5 ms later by the IPR event warning that the feedback control target plasma current request is no longer being met. By now, the original separatrix-limited plasma is in contact with the wall and is decreasing in size, with the edge plasma safety factor, q, decreasing as plasma poloidal flux is lost. At 9 ms later, a low q warning (LOQ) is issued. DIS occurs over 30ms after the trigger RWM is issued, which is expected to be just enough time in ITER to trigger the disruption mitigation system effectively. However, this relatively short-duration disruption chain would be better handled if the RWM event itself was forecast at an earlier time. DECAF presently has a model to do this, as discussed in Section 3.3.4. At present, DECAF event warning levels are determined by a flexible diagnostic and physics model "point" system similar to that successfully used for NSTX [6]. A key expansion of the present DECAF approach is that several event criteria can be used in conglomerate to determine combined "levels" that allow DECAF to issue event warnings. For example, at present, 15 separate criteria are used to determine the total MHD warning level for rotating MHD modes (see Section 3.2.1).

3. PHYSICAL MODEL DEVELOPMENT

A profound power of the DECAF approach is the ability to test any physical model developed by the fusion research community for practical use as part of a disruption prediction model ensemble. Models that can quantitatively forecast disruptions more accurately across all devices can then objectively be chosen as being more desirable. Over 50 disruption chain events are presently identified, with over 20 events that have diagnostic evaluation and physical models providing warning levels. Simpler evaluations examine key diagnostics in combination to compute warning levels, with comparison to critical levels to determine when DECAF issues event warnings. For example, the VDE event combines a comparison of axis position ($|Z|$), axis velocity ($|dZ/dt|$), and $Z\ dZ/dt$ against threshold levels set in the model. Critical levels of such models will differ for each machine. The validation of the technical and physics-based models for each of the 5 devices in the present DECAF database now comprises the primary near-term research effort. More desirable are models that more transparently reproduce the behaviour of all tokamak devices. The simplest models in this class are empirical models such as the Greenwald density limit. A next level includes models that are more closely based on first-principles physics, examples of which are discussed below.

3.1. Density limits

The Greenwald density limit [7] (event GWL) is included in DECAF as a universal empirical model for disruption forecasting. Recently several theories have been developed to explain the observed global Greenwald limit in tokamaks, including a ballooning stability limit at the separatrix [8] and a local island power balance theory [9,10]. In the latter theory, power balance in an island between input Ohmic heating and radiated power loss results in a maximum local density that scales with local current density. If the density at the island exceeds the limit, or alternatively if the radiated power at the island exceeds the input power ($P_{loss} > P_{input}$), then the island grows and can lead to plasma disruption. The limit can be written either in a form which mimics the global Greenwald density limit in a local form, or one that mimics a radiated power fraction localized to the magnetic island surface. This model has been added to the DECAF code including the radiated power, resistivity, and current density profiles as inputs.

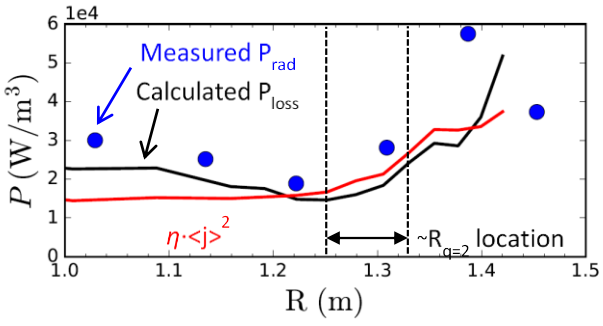

Fig. 2. Profiles of calculated (deuterium and carbon) and measured total radiated power density and calculated input power density for NSTX discharge 134020 at 0.60s.

The radiated power profile (P_{loss}) can either be measured directly or can be estimated from density profiles and calculated cooling rates of deuterium and impurities such as carbon, which depend on electron temperature [11]. Figure 2 shows both the measured and calculated profiles for an NSTX discharge. The P_{loss} is calculated as $P_{loss} = n_e \sum n_Z L_Z$, where the species Z considered in this case are limited to deuterium and carbon and the cooling rates L in Wm^3 are given for deuterium by $L_D = 5.35*10^{-37} T_e^{1/2}$ with electron temperature in keV [8], and for carbon by tabulated formulae in Ref. [11]. The input power profile which P_{loss} is compared to in Fig. 2 is calculated from $P_{input} = \eta j^2$. The resistivity profile, η, is calculated based on electron temperature and the

effective charge Z_{eff} (formula from Ref. [8]) which are measured by Thomson scattering and charge exchange recombination spectroscopy. The current density profile used here is the total surface-averaged current density profiles from various sources (Ohmic, bootstrap, beam-driven), which are computed by the TRANSP code.

The power balance model is a local condition for island growth, therefore mode marginal stability would occur when $P_{loss}/P_{input} > 1$ at the location of the island. This defines the DECAF event "island power balance" (IPB) shown in Fig. 2. The rotating MHD mode growth that arises when $P_{loss}/P_{input} = 1$ (Fig. 3) is measured as having toroidal mode number $n = 1$. The lowest order rational surface in the plasma is $q = 2$, so $m/n = 2/1$ activity is the most likely candidate. Therefore, the local power balance criterion is evaluated at the $q = 2$ surface. The $n = 1$ mode onset in Fig. 2 is highly correlated with the IPB event warning in the plasma shown. Also shown is the computed Greenwald fraction evolution and the DECAF event GWL defined as the line-averaged plasma density equal to the Greenwald density. At the IPB event, the Greenwald fraction is ~ 0.9. While this correlation is positive, the present state of analysis shows the quantitative evaluation of the IPB event to be sensitive to the accuracy of the local input criterion (e.g. position of the $q = 2$ surface). Present DECAF analysis shows that the local island power balance evolution follows the evolution of the global Greenwald fraction. For 13 discharges tested, the Greenwald fraction ranges from 0.75 to 1.05 at the time of MHD onset and the local island power balance fraction has a range of about 0.60 to 1.50. Continued analysis is focussed on reducing this variation and eliminating the need for full TRANSP analysis for each plasma, for example through neural net evaluation of a representative set of TRANSP runs to determine the required input for the IPB event.

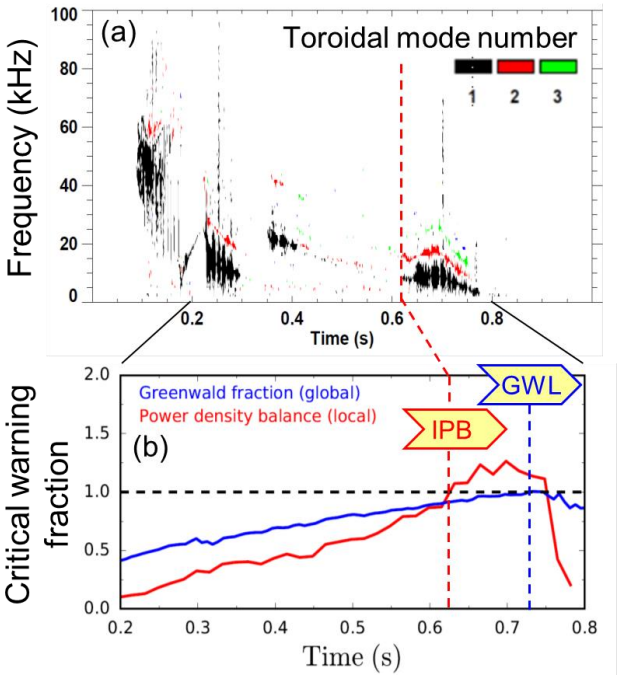

Fig. 3. (a) spectrogram of rotating MHD activity from a toroidal array of magnetic probes for NSTX discharge 134020, illustrating n = 1 mode growth near the time of the loss of power island power balance (DECAF event IPB), (b) Greenwald fraction and local power balance criterion.

3.2. Rotating MHD instabilities

Automated analysis of rotating MHD modes with tearing characteristics has started by using a DECAF module to produce physical event chains leading to disruptions through slowing of the modes by resonant field drag mechanisms and subsequent locking. An algorithm portable across tokamaks devices has been developed that processes the spectral decomposition and signal phase matching of magnetic probe signals for mode discrimination. Multiple modes occurring simultaneously are tracked and bifurcation of the toroidal rotation frequency and locking for each mode due to the loss of torque balance under resonant braking are detected.

3.2.1. Disruption Event Characterization

The information analysed for these modes along with plasma rotation profile and other plasma measurements produces predictive warnings for the individual modes, along with a total MHD event warning signal showing initial success as a disruption forecaster. These capabilities are illustrated in Figure 4 for the same plasma shown in Figure 3. In the plasma illustrated, rotating MHD instabilities thought to be non-linearly saturated and slowly evolving resistive modes are found using a generalized phase matching algorithm in DECAF using an array of toroidal magnetic probes typically available in tokamaks. The code discriminates the toroidal mode number of the instabilities and tracks all modes greater than a specified amplitude. Modes that approach the disruption are indicated by the chevrons in the diagram (which show the mode n number). DECAF events based on the mode evolution are also shown, including the bifurcation of the modes (BIF-n1,2) (loss of torque balance leading to rapid loss of mode rotation), and events marking the locking of the modes (LTM-n1,2). A single "total" MHD warning signal that varies with time is also shown. This warning is created by a set of criteria and can be used as a disruption predictor, as described in the next section.

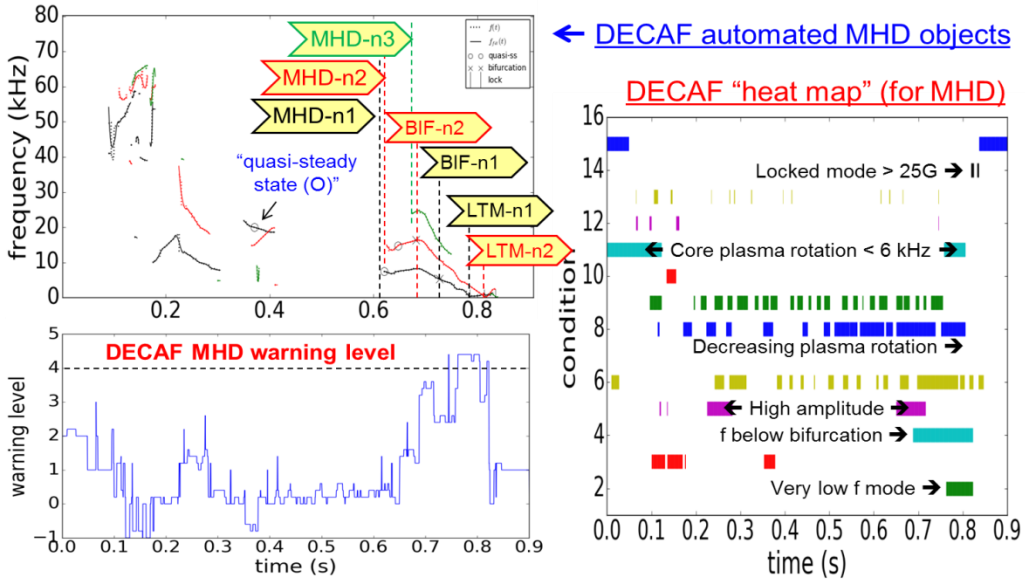

Fig. 4. Rotating MHD mode discrimination capabilities in DECAF. The upper left frame shows the mode discrimination and decomposition into DECAF events. The lower left panel shows a total MHD warning level that increases as the disruption is approached. The right panel shows a heat map illustration of 15 event criteria that comprise the total MHD warning level.

3.2.2. Forecasting

A significant part of DECAF research is determining the best criteria to create predictive warnings. The warning model shown in Fig. 4 is comprised of 15 separate criteria, also shown in the figure displayed as a heat map. This summary of model criteria provides a useful illustration of how the total warning level reaches high values, indicating a disruption onset. A total warning level of 4 indicates close proximity to the disruption for this model. The heat map also gives us an understanding of what is happening in the plasma to create the undesirable plasma states approaching the disruption. Early in the discharge, MHD modes are also found, and core plasma rotation is low as the plasma starts up and typically transitions from counter-NBI rotation to co-NBI rotation. However, the mode frequencies are relatively high at this time, which is generally a safe condition. Later, near t = 0.25s, the MHD warning level increases as modes are again found but now with decreased and decreasing rotation frequency. However, these frequencies are not critically low (no mode bifurcations are found) and plasma rotation is not low, so the warning level remains low. However, after t ~ 0.6s the heat map clearly shows more negative criteria occurring simultaneously including an increased mode amplitude, decreasing mode frequencies, and decreasing plasma rotation across the profile. Near t ~ 0.7s more negative criteria occur: mode frequencies are below past computed bifurcation frequency levels, the modes drop to very low frequency, and core plasma rotation is critically low. Late in the evolution in close time proximity to the disruption (t ~ 0.8s), a critical level of locked mode amplitude occurs. Such a locked mode detector signal is typically used to predict a possible disruption, but this indication occurs very late in the evolution. We see here that the DECAF analysis starts to show a significant change in the total MHD warning level about 180 ms earlier, providing far better advanced notice of the potential disruption allowing the potential for control systems to alter plasma stability to avoid disruption. Additionally, and of critical importance, the DECAF analysis provides physical understanding of the negative evolution of the plasma state as it moves toward the disruption. Further forecasting of resistive MHD stability using the resistive DCON code is being investigated through supporting KSTAR research [12].

3.3. Global MHD instabilities

Global MHD instabilities such as external kink/ballooning modes or RWMs [13] typically cause the most rapid disruptions (e.g. Fig. 1) and give the least amount of pre-disruption warning time. Therefore, attention needs to be put toward forecasting such events to cue profile control systems well before instability develops.

3.3.3. Disruption Event Characterization

To examine disruption event chains with global MHD triggers, DECAF analysis was performed on a database of 44 NSTX discharges that were pre-determined to have unstable RWMs which lead to disruptions. Tearing modes were stable during these discharges to focus on global MHD in this analysis. A typical disruption event chain with an RWM trigger was shown in Fig. 1. In this database, the RWM, loss of boundary control (WPC), LOQ, IPR, and DIS events are found in 100% of the plasmas, and VDE events are found in 91% of the plasmas.

The GWL event warning is found in a few cases when the warning level is set at a Greenwald fraction of 0.9. Interestingly, GWL can start the RWM disruption chain and is explained by the correlation of reduced plasma rotation caused by increasing plasma density, leading to RWM instability by a destabilizing change in the plasma rotation profile, discovered in NSTX [14]. Analysis shows that 61% of RWM events in a shot occur within 20 conducting wall current diffusion times, τ_w, of the disruption. The other RWM events found occur earlier but are not false positives as they cause significant thermal collapses or "minor disruptions" of the plasma with subsequent recovery (plasma stored energy can drop by 30% or more over tens of ms, much larger than the largest ELMs in tokamaks which cause far smaller stored energy decreases up to ~ 6%).

3.3.4. Forecasting

Kinetic RWM analysis has shown high success over years of quantitative comparison to experiment to determine the mode marginal stability allowed through plasma precession drift and bounce orbit resonances, collisionality, ν, and energetic particle effects [14,15]. To allow rapid processing, full kinetic RWM computations (using the MISK code [14,15]) that have been used successfully to predict mode stability on NSTX and DIII-D have been used to create a reduced model of the kinetic RWM stability growth rate in DECAF (Figure 5a). Gaussian functions with parameters fit from full MISK calculations of NSTX marginally stable equilibria are used to define the kinetic energy functional δW_K as functions of *ExB* frequency and collisionality. The model also incorporates expressions dependent on plasma pressure peaking, internal inductance, and aspect ratio for the ideal MHD no-wall and with-wall beta limits computed from thousands of DCON calculations using experimental equilibria [16].The modelled growth rate can be used to forecast RWM instability based on plasma equilibrium reconstructions and rotation measurements and is time-dependent based on the equilibrium evolution. Figure 5a) illustrates the evolution of a high normalized beta NSTX experimental plasma as it becomes RWM unstable near a predicted marginal stability contour (while not shown, the growth rate contours on Figure 5a change as the plasma evolves). This reduced kinetic RWM stability model in DECAF performed well in its first incarnation against a larger database of plasmas to determine the proximity of discharges to marginal stability (Figure 5b). The model predicted instability 84% of the time (stringent marginal stability evaluation) for experimentally unstable cases with a relatively low false positive rate. DECAF also showed 44% of plasmas were predicted unstable within 320 ms (~ 60 τ_w) of the disruption time, and 33% were predicted unstable within 100 ms of a minor disruption. Stability was predicted in 77% of experimentally stable cases. The evolution of discharges that were RWM stable were notably separate on the (ExB frequency, collisionality) stability map, not crossing the computed marginal stability contour.

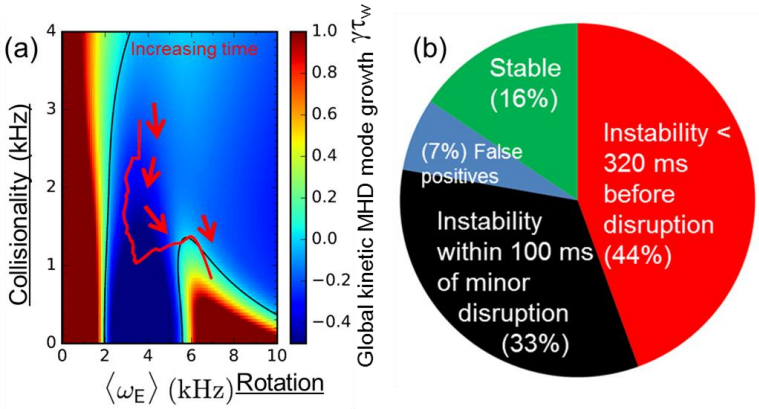

Fig.5. (a) Stability map vs. ExB frequency and collisionality from DECAF reduced kinetic RWM stability model; (b) statistics illustrating results of the model in forecasting instability for RWM unstable NSTX plasmas.

4. INITIAL INVESTIGATION OF GENERAL DATABASES

4.4. Individual disruption chain events

The DECAF code has recently produced an initial analysis of large databases for multiple tokamak devices for a small set of disruption characterization events. The analysis is conducted over the full duration of the planned plasma current flat-top, rather than a limited period near the disruption time as might be available from a disruption database. Thousands of shot seconds are available in the databases, with upwards of 0.5 – 1 million tested sample times per database. For example, if the DIS event is used, the analysis produces the equivalent of "disruptivity diagrams" showing the probability of a disruption occurring within a given parameter space of tokamak operation. These diagrams are shown for NSTX, MAST, and KSTAR in Figure 6 expressed as standard stability operational space (l_i,β_N) figures (l_i is the plasma internal inductance). This multi-device comparison illustrates a highly important and still largely unappreciated result separately published for DIII-D and NSTX [17] for smaller datasets that plasma disruptivity does not need to increase (and can actually

decrease) as β_N increases. However, as will be shown in the next section, the high beta regions of low disruptivity are in fact key areas for DECAF algorithms to analyse events that can lead to disruptions.

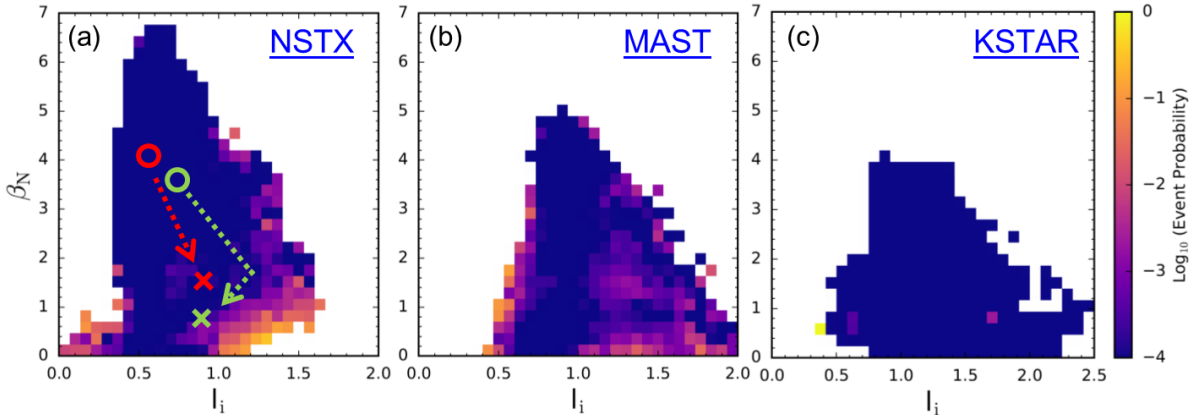

Fig. 6. Event probability diagram of DECAF event DIS during I_p flat-top showing that disruption probability does not have to increase as plasma normalized beta is increased based on large databases from the NSTX, MAST, and KSTAR tokamaks.

Unlike standard disruptivity plots, DECAF can provide additional insight by illustrating where in parameter space events other than DIS happen. For example, the VDE event detects the loss of vertical stability. When plotted in the parameter space of elongation, κ, vs. l_i, it becomes clear that vertical stability shows a strong dependence on these parameters (Figure 7a) and that, additionally, the location in parameter space of an event preceding the disruption (like VDE) can be far from where the actual disruption event occurs (DIS, shown in Figure 7b).

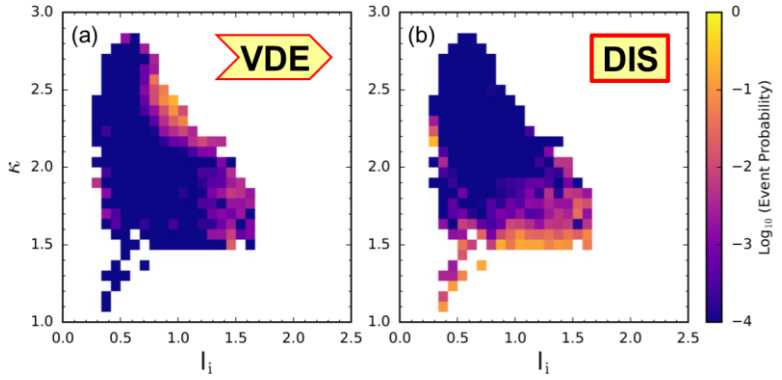

Fig. 7. Event probability diagrams of DECAF events VDE (a) and DIS (b) for a large database from the NSTX tokamak.

4.5. Disruption event chain analysis for arbitrary discharges

DECAF event characterization and event chain analysis shows that disruption forecasting analysis often start during plasma states that can appear safe. This is illustrated using the disruptivity database plot shown in Figure 6a) and the figures in this section. The regions of high disruptivity in Fig. 6a) may be thought to be the most important based on human inspection. However, an apparent problem is that the region of high disruptivity at low β_N and mid-range l_i is not physically understood to be a dangerous operational region. The enigma is resolved by understanding that the plasma state can evolve significantly from more usual high performance parameters to the point at which the disruption actually occurs. This fact is completely missed, for example, by disruption database studies that only process data near the disruption time. Even worse, such studies may parameterize disruptive limits based on these misguided terminal states. In contrast, DECAF disruption event chain analysis of two discharges in Fig. 6a) that disrupt (DIS event in DECAF, marked by red and green X's in the figure) show that the *start* of the event chains appears in the region indicated by the red and green circles – which are *far* from what might be expected. The disruption event chain for these plasmas in Figure 6 are shown in Figure 8 along with the DECAF MHD mode decomposition and total MHD warning level. As before, we see this warning level rising toward and past the critical value of 4.0 as the disruption is approached. The DECAF mode decomposition adds information showing that the mode evolution toward lower rotation frequencies is relatively slow. This is one reason why the plasma disrupts far from the plasma state at the trigger event.

The DECAF event chains in Figure 8 provide a wealth of information. In Fig. 8a), we see a critical warning for the individual n = 1 rotating MHD mode (MHD-n1) as a starting point for the chain. Note from the top frame that the low frequency n = 1 mode itself was detected far earlier – near t ~ 0.22s. However, the warning level for the activity was not determined to be sufficiently high then. The mode bifurcation (event BIF-n1) occurs 5 ms later. The mode locks (event LTM-n1) 45 ms after the bifurcation. Then, a different dynamic occurs, as DECAF finds a pressure peaking event warning (PRP) happening 23 ms later. While the warning literally flags that the

pressure peaking factor is exceedingly high, it also importantly indicates that an H-L energy confinement back-transition has occurred, the H-mode pedestal is lost, and the neutral beams have better penetration increasing the plasma pressure peakedness. The IPR warning occurs 5 ms after PRP and simultaneously the plasma is makes a close approach to the vessel wall (WPC). Finally, the plasma disrupts 4 ms after the WPC event. It is also interesting that the VDE event warning occurs 3 ms after DIS. Usually the events are reversed in time. This indicates that the plasma remains mainly on the midplane during the evolution, uncharacteristic of NSTX disruptions. Figure 8b) shows a relatively slow RWM-triggered disruption (i.e. compared to Fig 1b)). In this disruption event chain, the PRP warning again indicates an H-L back transition and a VDE is produced approximately $10\tau_W$ after the RWM trigger occurs. As shown, the disruptions in these two plasmas occur 77 ms and 101 ms after the initial DECAF warnings. These intervals represent transport timescales (a few energy confinement times) and so would allow sufficient time for active profile control for disruption avoidance, or easily allow time for active mode control or disruption mitigation.

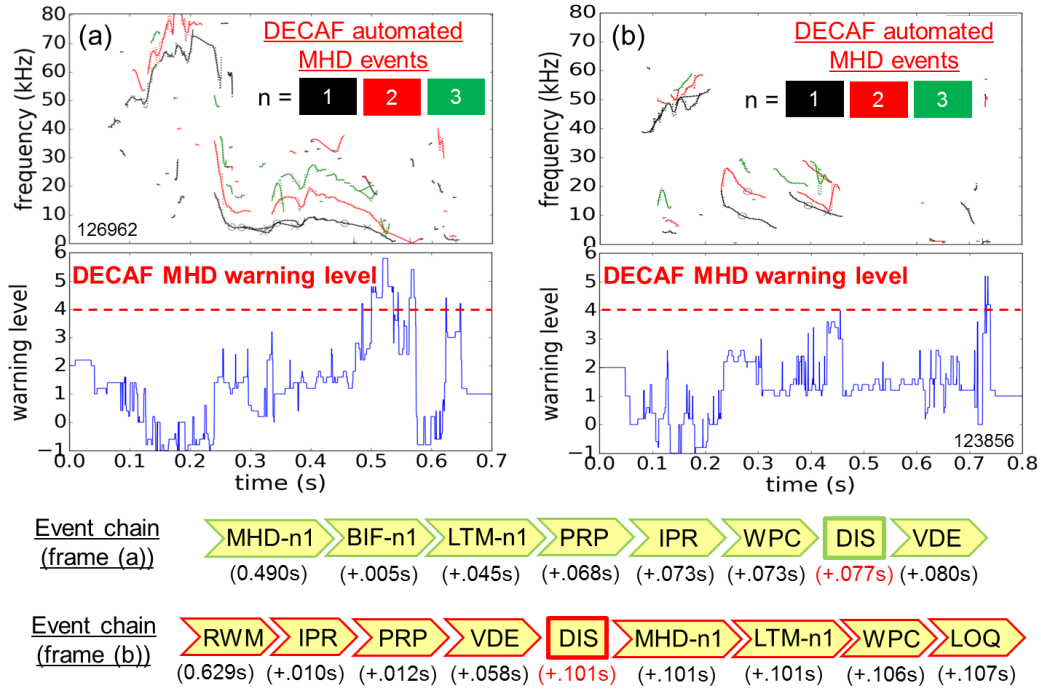

Fig. 8. (top to bottom) DECAF decomposition of rotating MHD in relatively slow evolutions toward disruption; total MHD warning signal; DECAF event chains leading to disruption. Plasma in frame (a) is triggered by rotating MHD, (b) by RWM.

ACKNOWLEDGEMENTS

This research is supported by U.S. DOE grants DE-SC0016614, DE-SC0018623, and DE-FG02-99ER54524.

REFERENCES

[1] HENDER, T.C., WESLEY, J.C., BIALEK, J., et al., Nuclear Fusion **47** (2007) S128.
[2] EIDIETIS, N. W., GERHARDT, S.P., GRANETZ, R.S., et al., Nuclear Fusion **55** (2015) 063030.
[3] SUGIHARA, M., et al. 2012 Proc. 24th Int. Conf. on Fusion Energy (San Diego, CA, 2012) ITR/P1-14, www-naweb.iaea.org/napc/physics/FEC/FEC2012/index.htm.
[4] DE VRIES, P.C., JOHNSON, M.F., ALPER, et al., Nuclear Fusion **51** (2011) 053018.
[5] SABBAGH, S.A., BELL, R.E., MENARD, J.E., et al., Physical Review Letters **97** (2006) 045004.
[6] GERHARDT, S. P., DARROW, D.S., BELL, R.E., et al., Nuclear Fusion **53** (2013) 063021.
[7] GREENWALD, M., TERRY, J.L., WOLFE, S.M., et al., Nuclear Fusion **28** (1988) 2199.
[8] EICH, T., GOLDSTON, R.J., KALLENBACH, A., et al., Nuclear Fusion **58** (2018) 034001.
[9] GATES, D. A. and DELGADO-APARICIO, L., Physical Review Letters **108** (2012) 165004.
[10] TENG, Q., BRENNAN, D.P., DELGADO-APARICIO, L., et al., Nuclear Fusion **56** (2016) 106001.
[11] POST, D. E., et al., Atomic Data and Nuclear Data Tables **20** (1977) 397.
[12] PARK, Y.S., SABBAGH, S.A., AHN, J.H., et al., (this conference), paper EX/P7-16.
[13] BONDESON, A. and WARD, D., Physical Review Letters **72** (1994) 2709.
[14] BERKERY, J.W. SABBAGH, S.A., BETTI, R., et al., Physical Review Letters **104** (2010) 035003.
[15] SABBAGH, S.A., BERKERY, J.W. BETTI, R., et al., Nuclear Fusion **50** (2010) 025020.
[16] BERKERY, J.W. SABBAGH, S.A., BELL, R.E., et al., Physics of Plasmas **24** (2017) 056103.
[17] BERKERY, J.W., SABBAGH, S.A., BALBAKY, A., Physics of Plasmas **21** (2014) 156112.